Crystallographic Features and Tetragonal Phase Stability of $PbVO_3$, a New Member of $PbTiO_3$ Family

Alexei A. Belik,*[,†,‡] Masaki Azuma,[†,‡] Takashi Saito,[†] Yuichi Shimakawa,[†] and Mikio Takano[†]

Institute for Chemical Research, Kyoto University, Uji, Kyoto-fu 611-0011, Japan, and PRESTO, Japan Science and Technology Agency, Kawaguchi, Saitama-ken 332-0012, Japan

Received September 16, 2004. Revised Manuscript Received October 28, 2004

Crystallographic features and stability of the tetragonal phase of $PbVO_3$ were investigated under ambient and high pressure and compared with those of $PbTiO_3$. $PbVO_3$ is isotypic with $PbTiO_3$ [at 300 K, space group *P*4*mm*; $a = 3.803\,91(5)$ Å and $c = 4.676\,80(8)$ Å, $Z = 1$]. Tetragonality (c/a) of $PbVO_3$ was the largest among the $PbTiO_3$-type compounds and increased monotonically with increasing temperature from 12 to 570 K without transition to cubic phase. The large tetragonality and the atomic position determined from synchrotron X-ray powder diffraction data suggest a large ferroelectric polarization above 100 $\mu C/cm^2$. Above 570 K in air, $PbVO_3$ was oxidized to $Pb_2V_2O_7$. Application of high pressure prevented the oxidation and thus a tetragonal-to-cubic phase transition accompanied by an insulator-to-metal phase transition was observed from about 2 GPa at room temperature.

1. Introduction

Ferroelectricity in ionic crystals is closely related to distortions of the crystal structure since the atomic displacement is the origin of the polarization. $PbTiO_3$ is a well-known ferroelectric with a large spontaneous polarization, P_s, of 81 $\mu C/cm^2$ at room temperature (RT). It has a perovskite-type tetragonal structure [space group *P*4*mm* ($Z = 1$)] at RT and a simple cubic perovskite structure above 763 K. Existence of the $6s^2$ lone electron pair of Pb^{2+} ion and the orbital hybridization between the Pb 6s state and O 2p states in $PbTiO_3$ play crucial roles[1] for the large tetragonal distortion ($c/a = 1.06$ at RT, where a and c are the lattice parameters) and large P_s among the related compounds, for example, $BaTiO_3$ ($P_s = 26\ \mu C/cm^2$ at RT)[2] and $KNbO_3$ ($P_s = 37\ \mu C/cm^2$ at 543 K).[3] Recently epitaxial thin film of $BiFeO_3$ was found to have a $PbTiO_3$-type structure and attracted much attention because $BiFeO_3$ has magnetic iron ions and possesses multiferroic properties.[4] Multiferroic materials, that is, those exhibiting two or all three of the properties (anti)-ferroelectricity, (anti)ferromagnetism, and ferroelasticity, have been studied intensively in recent years, for example, $YMnO_3$, $BiMnO_3$, $TbMnO_3$, and $TbMn_2O_5$,[5] in the expectation of their application to memory devices. However, the number of multiferroic materials is limited. Search for new multiferroic materials is essential work for the development of the field.[6]

A classical idea to realize a magnetic ferroelectric is to combine Bi^{3+} or Pb^{2+} with magnetic transition metal ions as in $BiFeO_3$ and $BiMnO_3$. $PbTiO_3$ is the only simple perovskite oxide with the composition $PbBO_3$ (*B* is a transition metal) which can be prepared at ambient pressure.[7] It is known that two other members, $PbCrO_3$ and $PbMnO_3$, can be obtained by high-pressure techniques. The former was reported to have a simple cubic perovskite structure,[8] and the latter a monoclinically distorted 6H hexagonal perovskite-type structure.[9]

Quite recently $PbVO_3$ was prepared by a high-pressure and high-temperature technique.[10] Its structure at RT was refined by use of laboratory X-ray powder diffraction data. $PbVO_3$ was found to be isotypic with $PbTiO_3$. Electronic properties of $PbVO_3$ were investigated by resistivity measurements and electronic structure calculations from first principles. We have also found this compound independently in the course of searching for new multiferroics.[11]

* To whom correspondence should be addressed. Present address: International Center for Young Scientists, National Institute for Materials Science, Namiki 1-1, Tsukuba, Ibaraki, 305-0044, Japan. Tel +81 (029) 851-3354 (ext. 8587); fax +81 (029) 860-4706; e-mail Alexei.BELIK@nims.go.jp.

† Institute for Chemical Research, Kyoto University.

‡ PRESTO, Japan Science and Technology Agency.

(1) (a) Cohen, R. E. *Nature* **1992**, *358*, 136. (b) Kuroiwa, Y.; Aoyagi, S.; Sawada, A.; Harada, J.; Nishibori, E.; Takata, M.; Sakata, M. *Phys. Rev. Lett.* **2001**, *87*, 217601.

(2) Kwei, G. H.; Lawson, A. C.; Billinge, S. J. L.; Cheong, S.-W. *J. Phys. Chem.* **1993**, *97*, 2368.

(3) Resta, R.; Posternak, M.; Baldereschi, A. *Phys. Rev. Lett.* **1993**, *70*, 1010.

(4) Wang, J.; Neaton, J. B.; Zheng, H.; Nagarajan, V.; Ogale, S. B.; Liu, B.; Viehland, D.; Vaithyanathan, V.; Schlom, D. G.; Waghmare, U. V.; Spaldin, N. A.; Rabe, K. M.; Wuttig, M.; Ramesh, R. *Science* **2003**, *299*, 1719.

(5) (a) Van Aken, B. B.; Palstra, T. T. M.; Filippetti, A.; Spaldin, N. A. *Nat. Mater.* **2004**, *3*, 164. (b) Kimura, T.; Kawamoto, S.; Yamada, I.; Azuma, M.; Takano, M.; Tokura, Y. *Phys. Rev. B* **2003**, *67*, 180401-(R). (c) Kimura, T.; Goto, T.; Shintani, H.; Ishizaka, K.; Arima, T.; Tokura, Y. *Nature* **2003**, *426*, 55. (d) Hur, N.; Park, S.; Sharma, P. A.; Ahn, J. S.; Guha, S.; Cheong, S.-W. *Nature* **2004**, *429*, 392.

(6) Hill, N. A. *J. Phys. Chem. B* **2000**, *104*, 6694.

(7) Glazer, A. M.; Mabud, S. A. *Acta Crystallogr., Sect. B: Struct. Sci.* **1978**, *34*, 1065.

(8) Roth, W. L.; DeVries, R. C. *J. Appl. Phys.* **1967**, *38*, 951.

(9) Bougerol, C.; Gorius, M. F.; Grey, I. E. *J. Solid State Chem.* **2002**, *169*, 131.

(10) Shpanchenko, R. V.; Chernaya, V. V.; Tsirlin, A. A.; Chizhov, P. S.; Sklovsky, D. E.; Antipov, E. V.; Khlybov, E. P.; Pomjakushin, V.; Balagurov, A. M.; Medvedeva, J. E.; Kaul, E. E.; Geibel, C. *Chem. Mater.* **2004**, *16*, 3267.

10.1021/cm048387i CCC: $30.25
Published on Web 12/22/2004

In this work, we report on the crystallographic and high-pressure behaviors of $PbVO_3$. $PbVO_3$ was found to be isotypic with $PbTiO_3$ between 12 and 570 K (space group *P*4*mm*). The structural properties of $PbVO_3$ in comparison with those of $PbTiO_3$ will be discussed, and other properties including thermal stability in air and resistivity and tetragonal-to-cubic (T-to-C) phase transition at high pressure will be presented. The tetragonal distortion is the largest in $PbVO_3$ among the reported $PbTiO_3$-type materials that suggests a large polarization of $PbVO_3$.

2. Experimental Section

$PbVO_3$ was prepared from a stoichiometric mixture of PbO, V_2O_5, and V_2O_3 by a high-pressure (HP) and high-temperature (HT) technique. The details of the HP cell used are described in ref 12. The mixture was sealed in a gold (or platinum) capsule and treated at 6 GPa and 973−1223 K (heating rate ~170 K/min) for 30−120 min, followed by quenching to RT. The samples for *P*−*E* (polarization vs electric field) hysteresis loop, resistivity, and specific heat measurements were prepared by pressing the obtained powders at 6 GPa without heat treatment since high density (about 97% of the theoretical density) was achieved by this method.

X-ray powder diffraction (XRD) data collected with a Rigaku RINT 2500 diffractometer (2θ range of 4−82°, step width of 0.02°, and counting time of 1 s/step) were used for phase identification. Low-temperature XRD data were recorded from 12 to 290 K on the same diffractometer.

Synchrotron XRD data of $PbVO_3$ for the structure refinement were measured at 90, 300, and 530 K on a large Debye−Scherrer camera at the BL02B2 beam line of SPring-8.[13] Incident beams from a bending magnet were monochromatized to $\lambda = 0.420\,87(9)$ Å. The sample was contained in a glass capillary tube with an inner diameter of 0.1 mm and was rotated during measurements. The synchrotron XRD data were collected in a 2θ range from 1° to 75° with a step interval of 0.01°. High-temperature synchrotron XRD data were collected between 300 and 850 K.

Synchrotron XRD experiments under HP were performed on the cubic anvil-type HP apparatus SMAP-2 installed at BL14B1 of SPring-8.[12] The data were collected by means of the energy-dispersive method with an SSD detector fixed at $2\theta \sim 4.5°$.

Thermal stability of $PbVO_3$ was examined under air with a MacScience TG-DTA 2000 instrument. The sample was placed in a Pt crucible, heated to 853 K, and cooled to RT with a rate of 10 K/min. *P*−*E* hysteresis loop measurements were performed with a standard Sawyer−Tower circuit. Dc electrical resistivity was measured at RT and HP by the two-probe method.

3. Results and Discussion

Almost single-phase samples of $PbVO_3$ were obtained by HP and HT technique. Although after the first HP−HT treatment, the samples contained small amount of $Pb_3(VO_4)_2$, PbV_6O_{11}, and some lead hydroxide carbonates (PDF 41−0677) as impurities, their quantity considerably decreased after the second HP−HT treatment at the same conditions described in the Experimental Section, and $Pb_3(VO_4)_2$ and PbV_6O_{11} were not detected. Reflections on the synchrotron XRD patterns were indexed in a tetragonal system with $a \approx 3.8$ Å and $c \approx 4.68$ Å. Since the lattice constants were consistent with those of a tetragonal perovskite structure and no systematic extinction conditions for reflection were found, we concluded that $PbVO_3$ is isotypic with $PbTiO_3$ having space group *P*4*mm* as it was determined in ref 10.

Structure parameters of $PbTiO_3$ were used as initial ones[14] in the Rietveld refinement of $PbVO_3$ by use of RIETAN-2000 software.[15] The Pb atom was placed at the origin (0, 0, 0). The occupancy factor, *g*, of all the sites was unity ($g = 1$). The isotropic Debye−Waller factor represented as $\exp[(-B \sin^2\theta)/\lambda^2]$ was assigned to all the sites, where *B* is the isotropic atomic displacement parameter. Partial profile relaxation[15] was applied to some broadened reflections to improve fits in these reflections in the last stages of the structure refinements. 2θ regions containing diffraction peaks from the impurities were excluded from the refinement since the structure of the present lead hydroxide carbonates is unknown.

Figure 1 shows experimental and calculated synchrotron XRD patterns of the Rietveld refinement for $PbVO_3$ at 300 K. The difference between the observed and calculated patterns are also shown at the bottom. Final lattice parameters and *R* factors are listed in Table 1. Fractional coordinates and *B* values for the final Rietveld analyses appear in Table 2 and selected bond lengths in Table 3. Rietveld analyses afforded sufficiently low *R* factors and reasonable *B* parameters for all the sites, suggesting that our structure analyses were successful. At 300 K, the simultaneous refinement of *g* and *B* parameters for Pb and V gave $g(\mathrm{Pb}) = 1.00(1)$ and $g(\mathrm{V}) = 1.00(1)$ [note that the refinement was very stable for cations with fixed $g(\mathrm{O1}) = 1$ and $g(\mathrm{O2}) = 1$]. This fact indicated that $PbVO_3$ had no noticeable cation deficiency. The refinement of the *g* parameters for oxygen atoms [with fixed *B* values for O1 and O2 as in Table 2 and with fixed $g(\mathrm{Pb}) = 1$ and $g(\mathrm{V}) = 1$] gave $g(\mathrm{O1}) = 0.98(2)$ and $g(\mathrm{O2}) = 0.98(2)$; that is, within standard deviations, the occupation of the oxygen sites is unity. Thus our structural analyses showed that $PbVO_3$ is a stoichiometric compound in agreement with the conclusion in ref 10.

It is interesting to compare the tetragonality (defined as the ratio of lattice parameters, *c*/*a*) and the degree of distortion for $PbTiO_3$ and $PbVO_3$. The *c* parameter in $PbVO_3$ is larger than that in $PbTiO_3$ while the *a* parameter in $PbVO_3$ is smaller than that in $PbTiO_3$, so the tetragonality is much larger for $PbVO_3$ ($c/a = 1.229$ at RT) in comparison with $c/a = 1.064$ for $PbTiO_3$.[14] The large *c*/*a* ratio in $PbVO_3$ can be explained by the large displacement of the O1 atom in the *z* direction ($\delta z_{O1} = 0.2102$) from the ideal position ($^1/_2$, $^1/_2$, 0) in comparison with that in $PbTiO_3$ ($\delta z_{O1} =$

(11) (a) Belik, A. A.; Azuma, M.; Takano, M. Meeting Abstracts of the Physical Society of Japan, 59th Annual Meeting, Kyushu University, March 27−30, 2004; Vol. 59, Issue 1, Part 3, p 510 (ISSN 1342−8349). (b) Azuma, M.; Niitaka, S.; Belik, A. A.; Ishiwata, S.; Kanda, H.; Yamada, I.; Takano, M. 4th International Conference on Inorganic Materials, Antwerp, Belgium, September 19−21, 2004; Elsevier: Amsterdam, 2004; Book of Abstracts, p 204
(12) Azuma, M.; Saito, T.; Ishiwata, S.; Yoshida, H.; Takano, M.; Kohsaka, Y.; Takagi, H.; Utsumi, W. *J. Phys.: Condens. Matter* **2002**, *14*, 11321.
(13) Nishibori, E.; Takata, M.; Kato, K.; Sakata, M.; Kubota, Y.; Aoyagi, S.; Kuroiwa, Y.; Yamakata, M.; Ikeda, N. *Nucl. Instrum. Methods Phys. Res. Sect. A* **2001**, *467*−*468*, 1045.
(14) Nelmes, R. J.; Kuhs, W. F. *Solid State Commun.* **1985**, *54*, 721.
(15) Izumi, F.; Ikeda, T. *Mater. Sci. Forum* **2000**, *321*−*324*, 198.

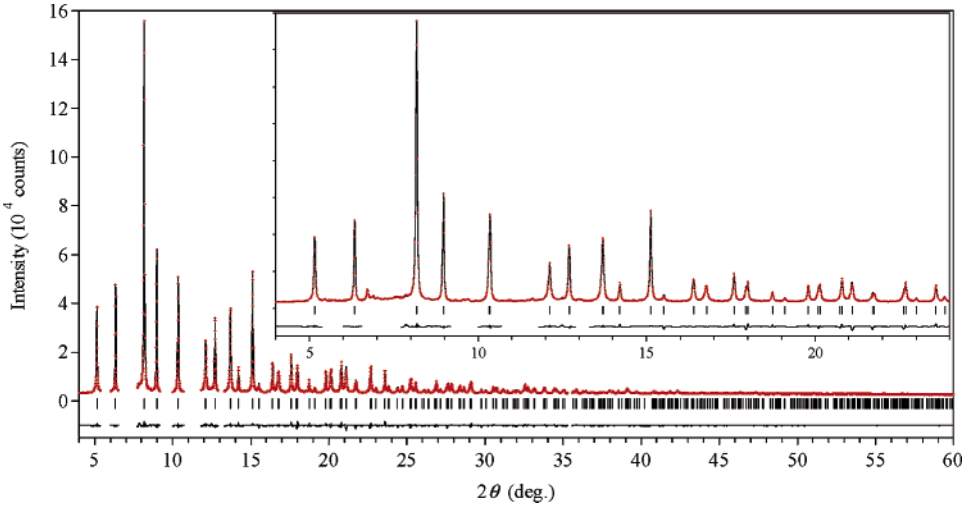

Figure 1. Observed (crosses) and calculated (solid line) synchrotron XRD patterns for $PbVO_3$ at 300 K. The difference pattern is shown at the bottom. Bragg reflections are indicated by tick marks. Inset presents the enlarge fragment with the full observed XRD pattern.

Table 1. Lattice Parameters and *R* Factors for $PbVO_3$ at 530, 300, and 90 K

T, K	*a*, Å	*c*, Å	R_{wp}, %	R_p, %	R_B, %	R_F, %	*S*
530	3.807 21(5)	4.698 19(9)	2.69	1.81	3.32	3.99	0.98
300	3.803 91(5)	4.676 80(8)	2.99	1.92	1.32	1.06	2.03
90	3.803 29(6)	4.649 89(10)	3.10	2.10	2.11	1.18	1.43

0.1118).[14] The reason of the large displacement of the O1 atom seems to be in the tendency of V^{4+} ions to form a strongly distorted octahedral coordination with one short vanadyl V−O distance (see Table 3), for example, as in $(VO)_2P_2O_7$.[16] The difference between two V−O1 distances, that is, distortion of the BO_6 octahedron [l(V−O1) = 1.668 Å and l(V−O1) = 3.009 Å], in $PbVO_3$ is much larger than the difference between Ti−O1 distances [l(Ti−O1) = 1.770 Å and l(Ti−O1) = 2.386 Å] in $PbTiO_3$.[14] Due to such a large difference in V−O1 distances, the coordination of V^{4+} ion is 5-fold. Thus the presence of V^{4+} ions plays a crucial role in a large tetragonal distortion in $PbVO_3$. The oxidation state of vanadium in the 5-fold coordination can be estimated from the equation $Z = 25.99-11.11l_{eq}$, where Z is the average valence and l_{eq} is the average equatorial bond distance.[17] With l_{eq} = 1.986 Å (Table 3), we obtained Z = 3.93.

Because of the extremely large tetragonal distortion, the polarization of $PbVO_3$ is also expected to be larger in comparison with other $PbTiO_3$-type compounds.[18] The rough estimation of P_s for $PbVO_3$ from the structural parameters at 300 K by use of the ionic model (for the equation see, for example, ref 2) was as large as 101 μC/cm^2. The estimation of P_s in $PbTiO_3$ by use of the same model gave P_s = 57 μC/cm^2. Note that the first-principle calculations with the Berry-phase approach supported the large P_s in $PbVO_3$ above 100 μC/cm^2. These data will be published elsewhere.[19]

Unfortunately, such a large structural distortion prevented the observation of $P-E$ hysteresis for $PbVO_3$. The measurement was performed up to an electric field of 90 kV/cm in liquid nitrogen but no hysteresis was observed. Above 90 kV/cm, the samples broke down. Note that the observation of a $P-E$ hysteresis loop in $PbTiO_3$ is possible only for the samples with resistivity above 10^{10} Ω·cm.[14,20] We could not reach such resistivity for our $PbVO_3$ samples. Resistivity depended on impurities, and maximum resistivity for the samples used in $P-E$ measurements was about 10^6 Ω·cm at RT. Note that, in ref 10, the resistivity at RT was reported to be only 10 Ω·cm.

No further distortion from the tetragonal symmetry was detected in the low-temperature XRD patterns of $PbVO_3$ down to 12 K, as in the case of $PbTiO_3$. Temperature dependences of lattice parameters are presented in Figure 2. In $PbVO_3$, the tetragonality increased with temperature from 12 to 570 K (inset of Figure 2). The change of the *a* parameter was very small, so the observed increase of tetragonality was mainly due to expansion in the *c* direction. This behavior of $PbVO_3$ is opposite to that observed in $PbTiO_3$, where the *c* parameter and the tetragonality decreases with increasing temperature and approaching to the T-to-C phase transition temperature in $PbTiO_3$.[21,22] The *a* parameter increases with temperature in both $PbVO_3$ and $PbTiO_3$. The behavior of $PbVO_3$ is unusual. However, the tendency for similar behavior was observed in $PbTiO_3$ at very low temperatures far below the T-to-C phase transition temperature.[21]

In the TG-DTA data, a weight gain of 2.5% was observed between 570 and 800 K. After the TG experiment, the resultant sample was checked by XRD and found to contain single-phased $Pb_2V_2O_7$. Thus $PbVO_3$ started to be oxidized in air above 570 K. The experimental weight gain was close to the calculated one of 2.6% (for the oxidation of $PbVO_3$ to $Pb_2V_2O_7$). This fact coupled with the structure refinement data confirmed the composition of $PbVO_3$ and showed that

(16) Koo, H.-J.; Whangbo, M.-H.; VerNooy, P. D.; Torardi, C. C.; Marshall, W. J. *Inorg. Chem.* **2002**, *41*, 4664.
(17) Schindler, M.; Hawthorne, F. C.; Baur, W. H. *Chem. Mater.* **2000**, *12*, 1248.
(18) Iniguez, J.; Vanderbilt, D.; Bellaiche, L. *Phys. Rev. B* **2003**, *67*, 224107.
(19) Uratani, Y.; Shishidou, T.; Ishii, F.; Oguchi, T. Private communication.
(20) (a) Gavrilyachenko, V. G.; Spinko, R. I.; Martynenko, M. A.; Fesenko, E. G. *Sov. Phys. Solid State* **1970**, *12*, 1203. (b) Tabata, H.; Murata, O.; Kawai, T.; Kawai, S.; Okuyama, M. *Jpn. J. Appl. Phys.* **1993**, *32*, 5611.
(21) Kobayashi, J.; Uesu, Y.; Sakemi, Y. *Phys. Rev. B* **1983**, *28*, 3866.
(22) Mabud, S. A.; Glazer, A. M. *J. Appl. Crystallogr.* **1979**, *12*, 49.

Table 2. Final Structural Parameters for $PbVO_3$ at 530, 300, and 90 K

	Pb 1*a* (0, 0, 0)		V 1*b* ($^1/_2$, $^1/_2$, *z*)		O1 1*b* ($^1/_2$, $^1/_2$, *z*)		O2 2*c* ($^1/_2$, 0, *z*)	
T, K	*B*, Å^2		*z*	*B*, Å^2	*z*	*B*, Å^2	*z*	*B*, Å^2
530	0.89(1)		0.5674(4)	0.63(5)	0.2102(15)	1.5(2)	0.6915(10)	0.9(1)
300	0.672(8)		0.5668(4)	0.49(4)	0.2102(16)	1.8(2)	0.6889(10)	1.2(1)
90	0.297(6)		0.5677(3)	0.17(3)	0.2087(15)	1.7(2)	0.6919(9)	0.4(1)

Table 3. Selected Interatomic Distances for $PbVO_3$ at 530, 300, and 90 K[a]

T, K	Pb−O1 × 4	Pb−O2 × 4	V−O1	V−O2 × 4	V−O1
530	2.868(3)	2.393(3)	1.678(8)	1.991(2)	3.020(8)
300	2.864(3)	2.395(3)	1.668(8)	1.986(2)	3.009(8)
90	2.859(2)	2.381(2)	1.669(7)	1.988(1)	2.981(7)

[a] All distances are given in angstroms.

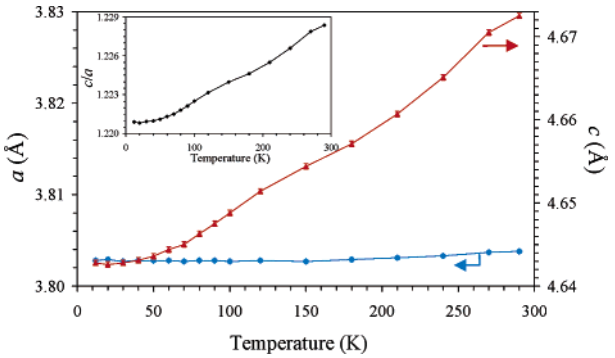

Figure 2. Temperature dependence of lattice parameters for $PbVO_3$ between 12 and 290 K. Inset shows the temperature dependence of tetragonality defined as *c*/*a*.

the average oxidation state of vanadium is +4. A high-temperature synchrotron XRD study showed that the tetragonal phase of $PbVO_3$ was still present from 570 to about 750 K; however, the quantity of impurities increased above 570 K. These data indicated that the temperature of T-to-C structural transition in $PbVO_3$ corresponding to the ferroelectric-to-paraelectric transition is above the decomposition temperature in air.

However, the cubic phase was realized at high pressure. Figures 3 and 4 depict the synchrotron XRD patterns taken at various pressures and temperatures. One experiment was done at RT and the pressure was changed from 0 to 5.9 GPa and then from 5.9 to 0 GPa (Figure 3). The second experiment was conducted at 2 GPa and the temperature was changed from RT to 773 K and then cooled to RT in 5 min (Figure 4). The relatively broad peak shapes in the latter are due to the Au capsule surrounding the sample to protect it from the strong reducing atmosphere generated by the carbon heater. Because the (101), (111), and (002) reflections of the tetragonal phase and (111) reflection of the cubic phase are not overlapped with other reflections, we mainly traced these peaks to check the appearance/disappearance of the tetragonal and cubic phases, respectively.

In the first experiment at RT, the peaks that can be assigned to the (110) and (111) reflections of the cubic phase (with $a \approx 3.9$ Å) appeared already at 2 GPa. The fraction of the tetragonal phase decreased with increasing pressure, but traces of (111) and (002) reflections of the tetragonal phase were still observed at 5.9 GPa. Thus the T-to-C phase transition in $PbVO_3$ takes place from about 2 to 5.9 GPa at RT. After the pressure was released, the (101) reflection of

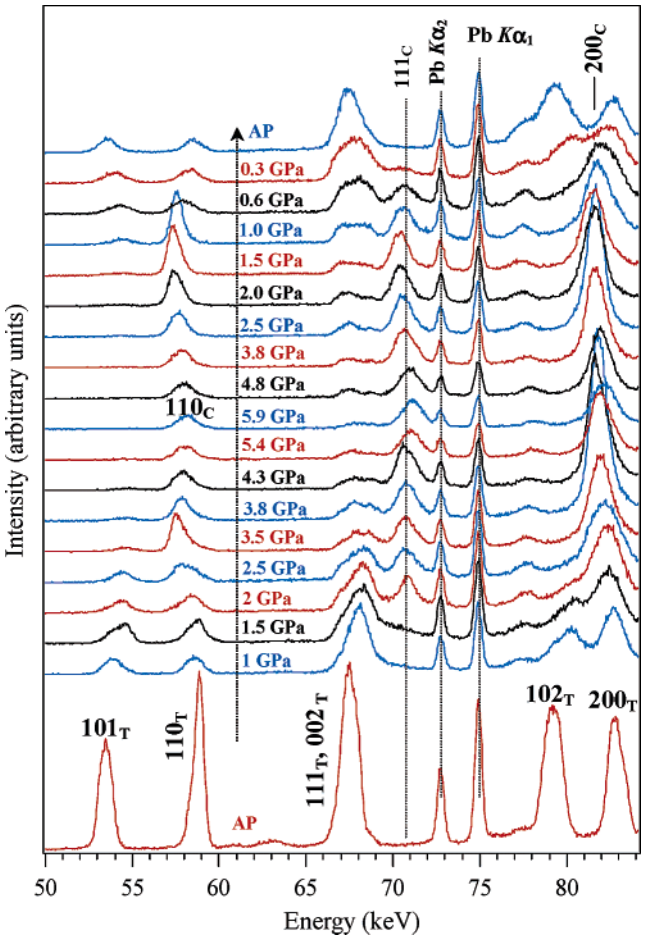

Figure 3. Energy-dispersive X-ray powder diffraction patterns for $PbVO_3$ at different pressure (at room temperature). (*hkl*) of the tetragonal (T) and cubic (C) phases are given.

the tetragonal phase appeared at ~2.0 GPa but the cubic phase was still present even at 0.3 GPa. The cubic phase disappeared only at ambient pressure. In the second experiment, the reflections of the tetragonal phase were still observed at 573 K and they completely disappeared only at 673 K and 2 GPa. After cooling from 773 K to RT at 2 GPa, the main phase was cubic. The cubic phase was still present at 1 GPa after the pressure was released and completely disappeared at ambient pressure and RT. The presence of very large hysteresis for the T−C phase transition indicates that this transition is first-order. The HP behavior of $PbVO_3$ is different from that of $PbTiO_3$, where the second-order T-to-C phase transition takes place from 11.2 GPa at RT.[23] In $BaTiO_3$, the T-to-C phase transition is of the first order and takes place between 1.8 and 3 GPa at RT.[24] Unfortunately, the resolution of our XRD data was low and

(23) Sani, A.; Hanfland, M.; Levy, D. *J. Solid State Chem.* **2002**, *167*, 446.
(24) Pruzan, Ph.; Gourdain, D.; Chervin, J. C.; Canny, B.; Couzinet, B.; Hanfland, M. *Solid State Commun.* **2002**, *123*, 21.

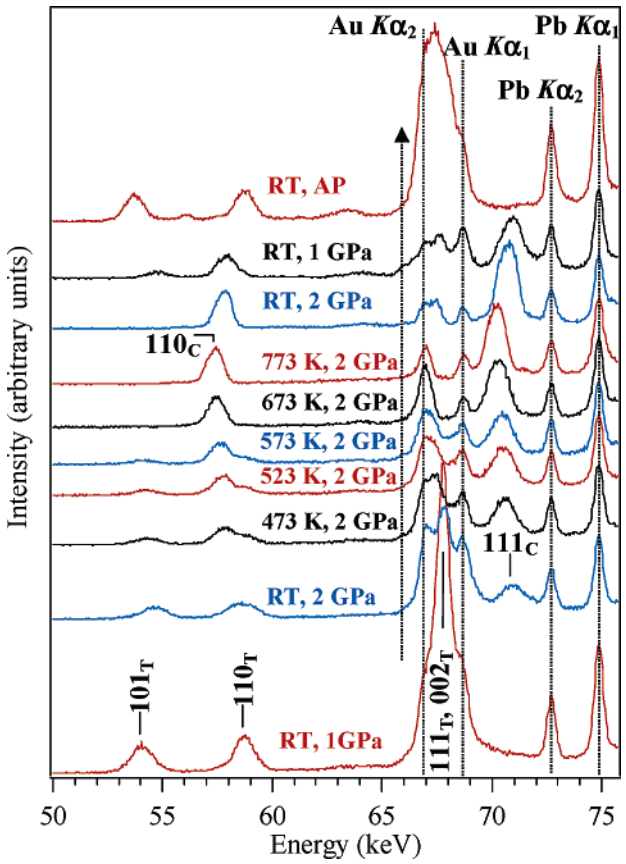

Figure 4. Energy-dispersive X-ray powder diffraction patterns for $PbVO_3$ at different pressure and temperatures. (*hkl*) of the tetragonal (T) and cubic (C) phases are given.

the number of the observed reflections was too small to obtain reliable pressure (temperature) dependence of lattice parameters in $PbVO_3$.

At this stage of the study, it is not clear whether the observed hysteresis in the high-pressure behavior of $PbVO_3$ was intrinsic or partially due to the deviatoric stress. Hydrostatic pressure experiments using a diamond anvil cell will provide further information about this pressure-induced structural transition in $PbVO_3$.

The pressure dependence of resistivity at RT is shown in Figure 5. A sharp decrease in resistivity was observed above about 2.5 GPa. With decreasing pressure, the sharp increase in resistivity was observed below about 1.5 GPa. This behavior of resistivity with large hysteresis agreed with the pressure dependence of the existence of the cubic phase (Figure 3). Even if the cubic phase appeared at 2 GPa, its fraction seemed not enough to cause the metallic conductivity. The metallic conductivity appeared only from 2.5 GPa. After the pressure is released, the cubic phase exists at very low pressure. The resistivity therefore returned to its starting

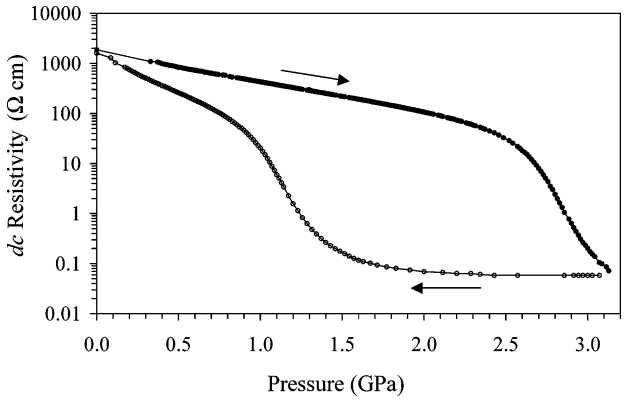

Figure 5. Pressure dependence of *dc* resistivity in $PbVO_3$ at room temperature.

value only at ambient pressure. These data gave us evidence to suggest that the cubic phase of $PbVO_3$ had metallic conductivity. Note that $SrVO_3$ at ambient pressure has the simple cubic perovskite structure and metallic conductivity.[25]

It should be noted that no anomaly characteristic of long-range magnetic ordering was found on magnetic susceptibility curves below 570 K down to 2 K and specific heat curves below 400 K down to 0.4 K. It is therefore reasonable to assume that $PbVO_3$ is an antiferromagnet with a Néel temperature higher than the decomposition temperature of 570 K. Detailed magnetic properties of this compound still need to be clarified. Note that the first-principle LSDA calculations predict the insulating ground state with antiferromagnetic ordering for $PbVO_3$.[10]

In conclusion, we investigated the crystallographic properties of $PbVO_3$ between 12 and 570 K and showed that the tetragonal phase of $PbVO_3$ was stable between 12 and 570 K. The tetragonality of $PbVO_3$ increased with increasing temperature in comparison with $PbTiO_3$. $PbVO_3$ has a very large tetragonal distortion in comparison with other $PbTiO_3$-type compounds that suggests a large polarization of $PbVO_3$. Structure parameters of $PbVO_3$ were refined from synchrotron XRD data at 90, 300, and 530 K. We have observed a pressure-induced insulator-to-metal transition associated with a tetragonal-to-cubic structural transition in $PbVO_3$.

Acknowledgment. The synchrotron radiation experiments were performed at the SPring-8 with the approval of the Japan Synchrotron Radiation Research Institute. We express our thanks to the Ministry of Education, Culture, Sports, Science and Technology, Japan, for Grants-in-Aid 13440111, 14204070, 12CE2005 for COE Research on Elements Science, and for 21COE on the Kyoto Alliance for Chemistry.

CM048387I

(25) Lan, Y. C.; Chen, X. L.; He, M. *J. Alloys Compd.* **2003**, *354*, 95.